FARADAY

Vibrational modes and structure of lanthanide fluoride–potassium fluoride binary melts

LnF_3–KF (Ln = La, Ce, Nd, Sm, Dy, Yb)

V. Dracopoulos,[a]† B. Gilbert[a]* and G. N. Papatheodorou[b]*

[a] *Laboratoire de Chimie Analytique B6, Universite de Liege, B-4000, Liege, Belgium*

[b] *Institute of Chemical Engineering and High Temperature Chemical Processes—FORTH and Department of Chemical Engineering, University of Patras, PO Box 1414, GR-26500, Patras, Greece*

Raman spectra of a series of LnF_3–KF (Ln = La, Ce, Nd, Sm, Dy, Yb) binary melt mixtures have been measured at temperatures up to 1000 °C and at compositions up to 40 mol.% for the mixtures with La and Ce and up to 25 mol.% for the remaining mixtures. The data indicate that at mole fractions $X_{LnF_3} \leqslant 0.25$ the LnF_6^{3-} octahedra are the predominant species giving rise to two main bands, one polarized, the other depolarized, which are assigned to the $\nu_1(A_{1g})$ and $\nu_5(F_{2g})$ vibrational modes of the octahedra, respectively. The ν_1 frequency varies almost linearly with the polarizing power of the lanthanide cation increasing from 445 cm^{-1} (Yb) to 400 cm^{-1} (La). Such a variation has not been observed in the corresponding binary melts involving chlorides and bromides; it is argued that the relative shielding of the Ln^{3+} by the anions are responsible for this behaviour. At mole fractions $X_{LnF_3} > 0.25$ the features of the reduced isotropic and anisotropic spectra are similar to those of the YF_3–KF (V. Dracopoulos, B. Gilbert, B. Børresen, G. Photiadis and G. N. Papatheodorou, *J. Chem. Soc., Faraday Trans.*, 1997, **93**, 3081). One polarized and two depolarized bands appear in the spectra which are interpreted to indicate that the predominant vibrations in these melts arise from distorted LnF_6^{3-} octahedra bound by common fluorides (edge sharing). The anisotropic scattering intensity was found to increase, relative to the isotropic intensity, with both increasing the size and mole fraction of the lanthanide cation. This unusual effect is attributed to dipole-induced-dipole interactions between cations in the melt and its variation from system to system is related to the size and polarizability of the Ln^{3+} cation and its relative shielding by the F^- anions.

Recently we have reported a systematic Raman spectroscopic study of the YF_3–KF and YBr_3–ABr (A = Li, K, Cs) binary melts.[1] Based on the changes of the vibrational modes with composition and temperature as well as the changes occurring upon melting crystalline compounds formed in the above binaries, it was concluded that the structural behavior of these melts is rather similar to that of the YCl_3–ACl melts.[2] In mixtures rich in alkali halide the YX_6^{3-} (X = F, Cl, Br) octahedra are the predominant species giving rise to two main bands assigned to the $\nu_1(A_{1g})$ and $\nu_5(F_{2g})$ vibrational modes of the octahedra. In molten mixtures rich in YX_3 four Raman bands are present whose polarization characteristics and energies suggest that the melt structure consists of D_3 distorted YX_6^{3-} octahedra bound by edges. Similar to this is the structure of the pure molten YX_3 component where a loose 'network' like structure is formed having edge bridged distorted octahedra. Thermodynamic data including enthalpies of mixing[3,4] and molar volume changes upon melting[5,6] as well as neutron diffraction measurements[7] support the proposed structures for both the binary melts and the YX_3 pure component.

The present work extends the above studies to a series of LnF_3–KF (Ln = La, Ce, Nd, Sm, Dy, Yb) binary melts. Due to experimental difficulties arising from the high melting points of the LnF_3 salts and the high corrosivity of the fluoride melts only the lower melting KF-rich compositions were studied. The measured spectra are correlated to the melt structure and the effects of binary composition, temperature and size of the lanthanide cation are examined and discussed.

Experimental

The lanthanide fluoride salts were purchased from Aldrich (LaF_3, CeF_3, NdF_3, DyF_3) and Alfa (SmF_3, YbF_3) and were of 99.9% purity. The salts were dried overnight under vacuum at 350 °C and were used with no further purification. The KF was purchased from Merck (99%) and was purified by slow crystallization from the melt. Vitreous carbon crucibles and an inert atmosphere furnace were used for the crystallization procedure. All room temperature operations for transferring the purified salts and filling the optical cells were carried out in closed fused silica containers and/or into a controlled Ar atmosphere glove box with a water content less than 5 ppm.

Graphite windowless cells were used to measure the Raman spectra at temperatures up to 1000 °C. The design of the cell and the experimental procedures used as described elsewhere.[8] All mixtures were premelted in a glassy carbon crucible in order to ensure homogeneity and then placed in the graphite windowless cells which were degassed under vacuum at 900 °C. A Spectra-Physics Model 2024 Ar ion laser was used to excite the spectra. The scattered light was collected at 90° and analyzed with a modified Cary 81 double monochromator equipped with a 9558 A EMI photomultiplier tube.[9] The spectrometer was interfaced with a personal computer (IBM PS/230) for recording the spectra and for calculating the isotropic and reduced Raman intensities.

Two polarization configurations were used for recording the melt spectra, vertical–vertical (VV) and horizontal–vertical (HV). The corresponding Raman intensities $I_{VV}(\omega)$ and $I_{HV}(\omega)$ at frequency shift ω were used to calculate the isotropic and anisotropic scattering from the relations:[1]

$$I_{ISO}(\omega) = I_{VV}(\omega) - \tfrac{4}{3}I_{HV}(\omega);\ I_{ANISO}(\omega) = I_{HV}(\omega) \qquad (1)$$

The reduced Raman intensity $R_\sigma(\omega)$, where σ stands for VV, ISO, HV (ANISO), is related to $I_\sigma(\omega)$ by:[1,10]

$$R_\sigma(\omega) = I_\sigma(\omega)\omega(\omega_0 - \omega)^4[n(\omega) + 1]^{-1} \qquad (2)$$

where ω_0 is the excitation laser frequency and $[n(\omega) + 1] = [\exp(h\omega c/kT) - 1]^{-1} + 1$ is the Boltzman

† Visiting Scientist from ICE/HT-FORTH

thermal population factor. The advantages for calculating and using the isotropic/anisotropic and the reduced representations for high temperature spectra are discussed elsewhere.[1,10]

Results and Discussion

The phase diagrams of the KF–LnF_3 binaries possess certain common characteristics.[11] In the KF-rich region the compounds K_3LnF_6 are formed having several allotropic crystalline forms.[12] One or two eutectics are formed at LnF_3 mole fractions less than 0.45. At LnF_3 mole fractions below 0.45 the liquidus temperatures for all systems are under 1000 °C while at mole fractions above this composition the liquidus temperatures increase rapidly towards the melting point of the LnF_3 salt.

The vapor pressure over the liquid mixture at *ca.* 1000 °C is rather small but slow attack of the vapors on the fused silica tube surrounding the graphite cell was observed and as a result the optical paths of the laser and scattered light were interrupted. Thus, both the high liquidus temperatures and the corrosivity of the fluoride vapors have limited our measurements at temperatures up to 1000 °C where the maximum mole fraction of LnF_3 is 0.4–0.5. The binaries LaF_3–KF and CeF_3–KF were studied at five different compositions up to 0.4 LnF_3 mole fraction while for the remaining systems the measurements were limited to the 0.25 and/or 0.1 LnF_3 mole fractions. Table 1 lists the composition and temperatures of all the binary systems for which Raman spectra were measured.

The spectra of all the LnF_3–KF mixtures at LnF_3 mole fractions 0.1 and 0.25 are rather similar possessing a well defined polarized and a depolarized shoulder band at frequencies noted in Table 1. Fig. 1 shows the spectra for the $X_{LnF_3} = 0.25$ mixtures for all the systems studied including the corresponding spectra of the YF_3 mixture reported in ref. 1. The polarization characteristics, the values of the frequencies measured and their proximity to the frequency of the YF_6^{3-} octahedra[1] are interpreted to indicate that the predominant species in all these KF-rich binary mixtures are the LnF_6^{3-} octahedra. The polarized and depolarized bands are assigned to the $\nu_1(A_{1g})$ and $\nu_5(F_{2g})$ vibrational modes of the octahedra, respectively. The ν_1 stretching frequency is in the range 400–450 cm^{-1} and its value increases almost linearly with the polarizing power of the Ln cation. This is shown in Fig. 2 where the ν_1 octahedra frequency of the fluorides is compared with that of the corresponding chlorides[2,13] and bromides.[1,14] It seems that in contrast to the fluorides the ν_1 frequency of the other two halides does not change drastically with the Ln cation size. This is presumably due to the relative sizes of the anions and cations involved in the formation of the LnX_6^{3-} octahedra. The radius of the octahedral hole created by six (spherical) anions in contrast is $r^*_{max} = 0.41\ r^-$, where r^- is the radius of the anion. For the octahedral species involving the large anions Br^- ($r^-_{Br} = 1.96$ Å)[15] and Cl^- ($r^-_{Cl} = 1.81$ Å)[15] most of the lanthanide cations fit into the octahedral site with small steric hindrance and consequently shielding of the cation occurs. Thus, the anion–anion distance is not affected much by the lanthanide and the overall size of the octahedra remains almost constant. In turn breathing $\nu_1(A_{1g})$ mode will not be influenced much by the central cation and its energy (frequency) will change slightly along the lanthanide series. In contrast, the smaller fluoride ($r^-_F = 1.33$ Å)[15] anions participating in the LnF_6^{3-} octahedra do not shield very effectively the central cation and thus, the $\nu_1(A_{1g})$ breathing vibration depends on the size of the central Ln^{3+} cation which is in contact with the anions and determines the F^-–F^- distance.

The depolarized band $\nu_5(F_{2g})$ is broad for all systems and is superimposed on the tail of the low frequency region (liquid wing) of the spectra (Fig. 1). The scattering intensity in this region was found to increase relative to the $\nu_1(A_{1g})$ band with

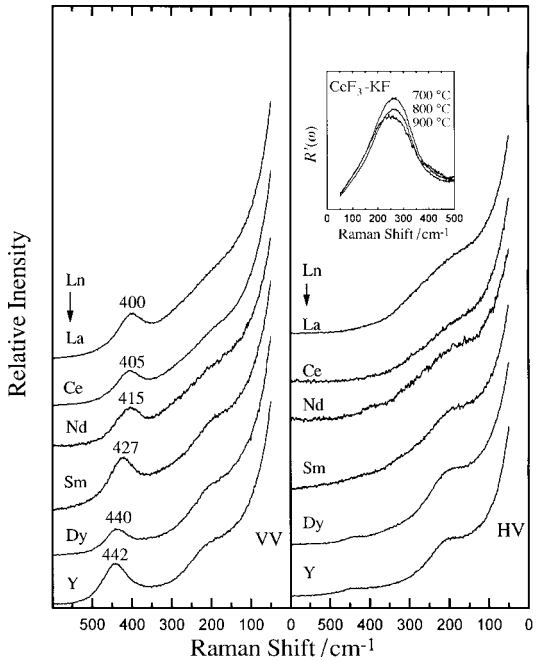

Fig. 1 Raman VV and HV spectra of 0.25 LnF_3–0.75 KF melts. Temperature: for Nd melts 850 °C, for all other melts 1000 °C. Inset: Temperature dependence of the relative reduced anisotropic spectra of 0.2 CeF_3–0.8 KF molten mixture. $R'(\omega)$ denotes the anisotropic intensity relative to that of the isotropic. Laser wavelength, $\lambda_0 = 488$ nm; spectral slit width, $w \approx 5$–6 cm^{-1}; time constant $\tau = 0.1$ s; scan rate = 500 cm^{-1} min^{-1}.

Table 1 Main reduced Raman frequencies in the LnF_3–KF (Ln = La, Ce, Nd, Sm, Dy, Yb) mixtures at different composition and temperatures

composition (mol.% LnF_3)	temperature/°C	frequencies/cm^{-1} [a,b,c] P	D_1	D_2
LaF_3–KF				
10%	850	406	244	
	1000	408	242	
20	1000	409	240	
25	1000	408	260	
30	1000	409	(242)	287
40	1000	411	(242)	296
CeF_3–KF				
10	850	412	240	
	1000	412	232	
20	700	411	266	
	800	412	265	
	900	413	249	
	1000	414	229	
25	1000	412	239	
30	1000	414	(232)	283
40	1000	415	(232)	302
NdF_3–KF				
10	850	419	220	
25	850	420	264	
SmF_3–KF				
10	850	428	223	
25	1000	428	226	
DyF_3–KF				
10	850	442	223	
	1000	442	231	
25	1000	443	232	
YbF_3				
10	850	456	229	
	1000	455	231	

[a] Frequencies with an estimated error of 1 cm^{-1}. [b] Numbers in parentheses indicate shoulder bands and frequencies with an estimated error of 10 cm^{-1}. [c] The frequencies of the bands were calculated from the spectra using eqn. (1) and (2). The isotropic band is marked as P and the anisotropic bands as D_1 and D_2.

increasing size of the Ln^{3+} cation. As will be discussed below this effect is also related to the cation shielding by the anions, the overall size of the octahedra and the polarizabilities of the cations involved.

The temperature dependence of the spectra was studied for CeF_3–KF near the eutectic with $X_{CeF_3} \approx 0.2$ in the range 700–1000 °C. For this composition the spectra were found not to change drastically with temperature. A weak softening of the well defined $\nu_1(A_{1g})$ band and an increase of its half width with increasing temperature were observed. These changes are expected and reflect the stability and the lifetime of the octahedral species formed in the melt mixture.[16] It was further observed that with increasing temperature the reduced intensity of the anisotropic $\nu_5(F_{2g})$ band decreases relative to that of the isotropic $\nu_1(A_{1g})$ band (see inset Fig. 1). This variation will be further discussed at the end of the present discussion.

The spectra of the LaF_3–KF and CeF_3–KF systems were measured at compositions up to $X_{LnF_3} = 0.4$. Fig. 3 shows the reduced isotropic and anisotropic spectra of these two binaries at $X_{LnF_3} = 0.1$, 0.3 and 0.4 and compares them with the corresponding YF_3–KF binary mixture. LaF_3 and YF_3 represent in many respects the two 'ends' in the lanthanide (rare earth) series having the cations with the largest (r_{La}^{3+} = 1.03 Å) and one of the smallest (r_Y^{3+} = 0.9 Å) radii.[15] All other systems (except Yb) lie in between and their spectra show an intermediate behavior as documented in Fig. 1–3. The isotropic spectra in Fig. 3 show a strong main band (P) at all compositions and for all systems. The systematics presented in ref. 1 and 14 have shown that an isotropic P band is present in all LnX_3–AX binaries studied so far and that the P band is composed of two overlapping isotropic bands P_1 and P_2. For the yttrium binaries involving chlorides and bromides[13,14] the two P_1, P_2 bands split; the location of P_1 remains constant at all compositions (up to pure LnX_3 melts) and the P_2 shifts relative to P_1 with increasing lanthanide halide mole fraction. The splitting and frequency shift increase in the sequences F → Br and La → Y. For the YF_3–KF system studied up to 50% the P_1 and P_2 bands overlap and their presence can be recognized only at $X_{YF_3} = 0.5$ which was the maximum composition studied. As a consequence of these systematics we suggest that the P band observed in the LaF_3–KF and CeF_3–KF binaries is also composed of two overlapping bands. However, the positions of these bands remain practically unchanged with composition indicating that the Ln–F stretching frequency of the LnF_6^{3-} octahedra is preserved in these melts at compositions up to 40 mol.% which was the composition limit of our experiments.

The anisotropic spectra show also the systematic changes observed previously for the YF_3–KF and LnX_3–KX (X = Cl, Br) systems. As the LaF_3 (or CeF_3) mole fraction increases the $\nu_5(F_{2g})$ anisotropic band (D_1) is overcome by a new anisotropic band (D_2) at higher energies (Fig. 3). As was argued for the YF_3–KF binary[1] the presence of both the isotropic P (or P_1, P_2) band and the two anisotropic D_1 and D_2 bands sug-

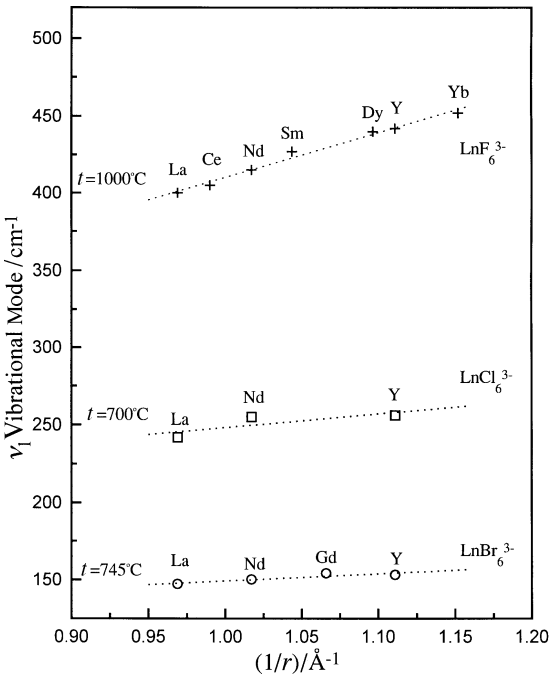

Fig. 2 The ν_1 frequency of the LnX_6^{3-} *vs.* inverse of Ln^{3+} ionic radius

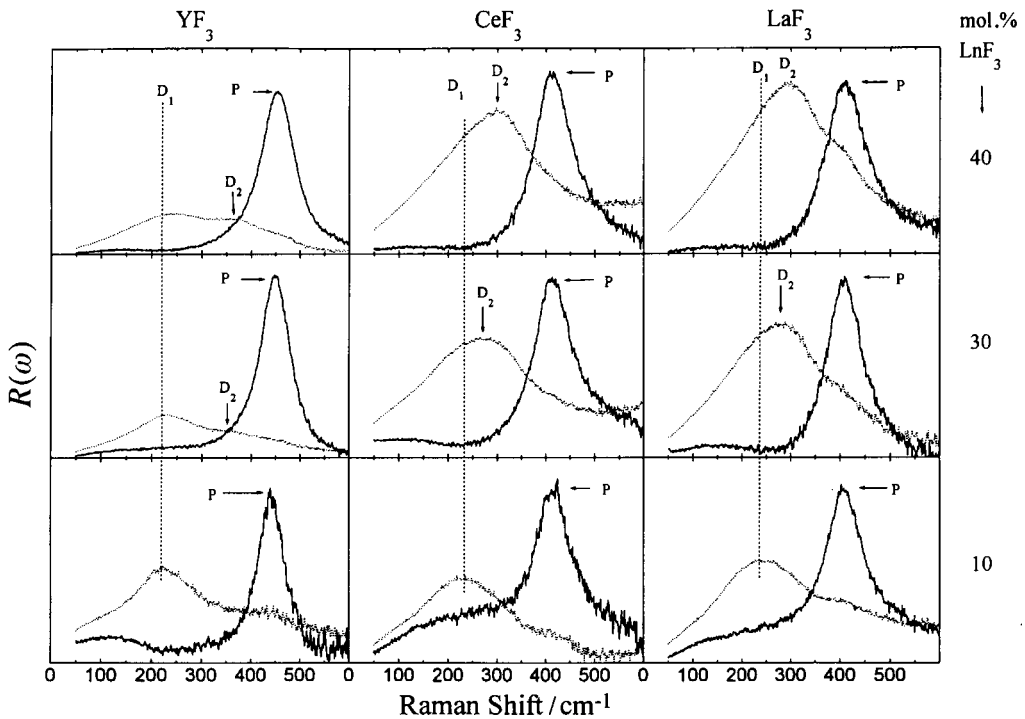

Fig. 3 Composition dependence of the reduced isotropic (——) and anisotropic (·····) Raman spectra of the molten KF–LnF_3 (Ln = Y, Ce, La) at 1000 °C. Spectral conditions are as in Fig. 1.

gests that the predominant vibrational modes in the LaF_3 (or CeF_3)-rich mixtures arise from the D_3 distortions of the LaF_6^{3-} octahedra bound by edges in melts with $X_{LaF_3} > 0.25$. Above this mole fraction the lanthanides are forced to share common fluorides and start to create loose structures of bridged octahedra. The presence of the P (P_1, P_2), D_1 and D_2 bands in all systems shown in Fig. 3 indicates that the structure of the two 'end' cases of melts containing LaF_3 and YF_3 are not different and presumably all intermediate lanthanide fluoride melts have similar structural behavior.

A rather new feature of the spectra is the variation of the intensity of the anisotropic scattering (Fig. 3). The substitution of Y with La increases rather rapidly the R_{ANISO} intensity. This is observed in the LnF_3–KF-rich melts and is very pronounced in the $X_{LnF_3} = 0.4$ mixtures where the anisotropic scattering intensity especially for the LaF_3–KF mixture is comparable to that of the isotropic scattering intensity. It should be pointed out here that strong anisotropic scattering has been found recently[17] in other ionic systems involving highly polarizable ions. Thus, the anisotropic scattering intensity from molten CsCl is higher than that of the isotropic, while the opposite occurs for the scattering from molten LiCl. A justification of this feature was given based on the polarizabilities and size of the cations involved and it was argued that polarizability fluctuations mainly due to dipole-induced-dipole (DID) interactions between neighboring Cs cations give rise to the strong anisotropic scattering observed for the CsCl melts.[17]

In mixtures where the LnF_6^{3-} octahedra are bridged the lanthanide cations come close to each other. Depending on the size of the lanthanide (see Fig. 4) there is a variation of the space defined between the outer electrons of both the bridging fluorides (distance σ) and the neighboring cations (distance σ'). Thus, for bridged lanthanum octahedra $\sigma = 0.81$ and $\sigma' \approx 1.26$ while at the other end of the series the yttrium octahedra have $\sigma = 0.5$ and $\sigma' \approx 1.38$. In other words the space allowing DID interaction is more favorable for La than for Y. Furthermore, the polarizability of La^{3+} is about double than that of Y^{3+}.[18] It seems that the smaller σ' and the higher polarizability of La^{3+} allows stronger DID interactions between the neighboring La^{3+} ions and thus, the intensity of the depolarized scattered light increases relative to that of the corresponding yttrium system.

For the fluoride systems the increase of the lanthanide size increases the cation polarizability and decreases the σ' distance. This in turn enhances the DID interactions and gradually increases the anisotropic scattering intensity. On the other hand, as it was mentioned before, for the chloride and bromide systems the Ln^{3+} cations are well shielded by the anions, the σ is rather small and the distance σ' between cations increases; thus the DID interactions do not contribute to the anisotropic scattering and the R_{ANISO} to R_{ISO} relative intensity does not change as we go either from Y to La or from Cl to Br.

In the KF-rich mixtures the LnF_6^{3-} octahedra have the K^+ cations as nearest neighbors thus, weak DID interactions may also arise between the Ln^{3+} partially shielded by the fluorides and the mobile K^+. These interactions increase with increasing the size of the lanthanide cation and contribute to the depolarized scattering intensity. In other words as the shielding of the lanthanide decreases along the series the depolarized light intensity is expected to increase; this is in agreement with the experimental findings mentioned earlier in this section and enhances the view that polarizability fluctuation due to DID interactions contributes to the anisotropic light scattered by these melt mixtures.

Finally, a further support attributing the strong depolarized scattering from the fluoride systems to DID interactions is given by the temperature dependence of the D_1 band reduced intensity relative to that of the P band measured in the 0.20 CeF_3–0.80 KF binary (Fig. 1, inset). With increasing temperature a decrease of the reduced depolarized scattering intensity is observed, an effect which has been also observed in the case of the CsCl melts and is attributed to diminishing DID polarizability fluctuations with increasing temperature.[17]

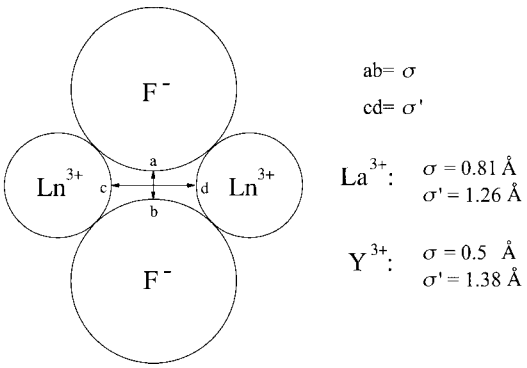

Fig. 4 Relative spaces between near neighbor ions

References

1 V. Dracopoulos, B. Gilbert, B. Børresen, G. Photiadis and G. N. Papatheodorou, *J. Chem. Soc., Faraday Trans.*, 1997, **93**, 3081.
2 G. N. Papatheodorou, *J. Chem. Phys.*, 1977, **66**, 2893.
3 G. N. Papatheodorou, O. Waernes and T. Ostvold, *Acta Chem. Scand., Sect. A*, 1979, **33**, 1799.
4 K. C. Hong and O. J. Kleppa, *J. Phys. Chem.*, 1979, **78**, 178.
5 K. Igarashi and J. Mochinaga, *Z. Naturforsch*, 1987, **42a**, 777 and references therein.
6 A. D. Kirshenbaun and J. A. Cahill, *J. Chem. Eng. Data*, 1962, **7**, 98.
7 M. L. Saboungi, D. L. Price, C. Scanehorn and M. P. Tosi, *Europhys. Lett.*, 1991, **15**, 283.
8 B. Gilbert, G. Mamantov and G. M. Begun, *Appl. Spectrosc.*, 1975, **29**, 276.
9 B. Gilbert and T. Materne, *Appl. Spectrosc.*, 1990, **44**, 299.
10 O. Faurskov Nielsen, *Annu. Rep. Prog. Chem. Sect. C, Phys. Chem.*, 1994, **91**, 3.
11 *Phase Diagrams for Ceramists*, ed. L. B. Cook and H. F. McMurdie, American Ceramic Society, Westerville, OH, vol. 7, 1989.
12 L. P. Reshetuskova, I. B. Shaimuradov, V. E. Efremov and A. V. Novoselova, *Dokl. Akad. Nauk. SSSR*, 1973, **213**, 98.
13 G. M. Photiadis, G. A. Voyiatzis and G. N. Papatheodorou, *Molten Salts Forum*, 1993/94, **1/2**, 183.
14 B. Børresen, V. Dracopoulos, G. M. Photiadis, B. Gilbert and G. N. Papatheodorou, *Proceedings of 10th International Symposium of Molten Salts*, ed. R. T. Carlin, S. Deki, M. Matsunaga, D. S. Newman, J. R. Selman and G. R. Stafford, The Electrochem. Soc. Inc., Pennington, NJ, 1996, vol. 96–7, p. 11.
15 R. D. Shannon, *Acta Cryst.*, 1976, **A32**, 751.
16 H. M. Brooker and G. N. Papatheodorou in *Advances in Molten Salt Chemistry*, ed. G. Mamantov, Elsevier, New York, 1983, vol. 5, p. 27.
17 G. N. Papatheodorou, S. G. Kalogrianitis, T. G. Mihopoulos and E. A. Pavlatou, *J. Chem. Phys.*, 1996, **105**, 2660.
18 J. R. Tessman, A. H. Kahn and W. Shockley, *Phys. Rev.*, 1953, **92**, 890.

Paper 8/02812E; *Received* 15*th April*, 1998